Int J Syst Assur Eng Manag (August 2019) 10(4):836–847
https://doi.org/10.1007/s13198-019-00818-5

ORIGINAL ARTICLE

Fault diagnosis for gearbox based on EMD-MOMEDA

Xin Zhang[1] · Jianmin Zhao[1] · Xianglong Ni[2] · Fucheng Sun[2] · Hongyu Ge[3]

Received: 22 March 2018 / Revised: 16 May 2019 / Published online: 15 June 2019

Abstract In this paper, a new method for fault detection of parallel shaft gearbox based on the Empirical Mode Decomposition (EMD) and Multipoint Optimal Minimum Entropy Deconvolution (MOMEDA) is proposed. MOMEDA can overcome the shortcomings of minimum entropy deconvolution (MED) and Maximum Correlated Kurtosis Deconvolution (MCKD), and it is introduced to extract the fault cycle of gearbox signals. The vibration signals of gearbox are complex, including fault signals, noise signals and deterministic signals such as gear meshing component. Fault signal is often buried in these other components, which increases the difficulty of gearbox fault detection. Thus the EMD is proposed to decompose the signal and extract the fault impact components from the signal. The parallel shaft gearbox preset fault experiment is carried out to verify the effectiveness of method. In addition, some traditional methods, such as Fourier transform, cepstrum analysis, MED and MCKD, are used to compare with the proposed methods. Experimental results show that the effectiveness of the proposed method is better than that of traditional methods.

Keywords Gearbox · Fault diagnosis · EMD · MOMEDA · Signal processing

✉ Xin Zhang
zxyx361@163.com

[1] Army Engineering University, Shijiazhuang, China

[2] Luoyang Electronic Equipment Test Center of China, Luoyang, China

[3] Baicheng Ordnance Test Center, Baicheng, Jilin, China

1 Introduction

The parallel shaft gearbox is one of the most vital and common component of rotating machinery. It is widely used in some rotating machinery such as automobile, power generating turbines, helicopters and more. The faults of gearbox are common cause of rotating machinery breakdown, and it can generally result in financial losses even safety accidents. Therefore, gearbox fault detection plays an important role in preventing breakdown accidents of rotating machinery and reducing economic losses (Samuel and Pines 2005). When faults occur on gearbox, fault signals with periodic impact components will be generated during gearbox operation. These impulsive components in the vibration signal appear in a fixed period and form a fixed frequency, which is the fault frequency (Golafshan and Sanliturk 2015). The vibration signal analysis is a common and effective method for gearbox fault detection (McFadden and Smith 1985). Several signal analysis techniques have been employed for gearbox fault detection, such as acoustic emission technology, infrared thermal imaging technology and oil analysis technology. Gu et al. (2011) used Discrete Wavelet Transform (DWT) and envelope analysis to analyze the collected acoustic emission signals, and achieved the purpose of gearbox fault diagnosis. Lim et al. (2014) combines infrared thermal imaging technology with Support Vector Machine (SVM) to diagnose faults of rotating machinery. Hamilton and Quail (2011) summarized the oil analysis technology used in wind turbine gearbox. However, acquisition of acoustic emission signals requires a higher sampling frequency, resulting in a huge amount of data, which limits the engineering application. Infrared thermal imaging technology and oil analysis technology are more suitable for monitoring the running state of equipment, and the accurate fault detection of rotating machinery is still in the exploratory stage.

The traditional vibration analysis methods of gearbox fault diagnosis include time domain analysis (McFadden 1991; Enayet et al. 2008; Hong and Dhupia 2014) and frequency domain analysis (Feng et al. 2016; Hong and Dhupia 2014). However, the raw vibration signal of gearbox contains non-stationary and non-linear components, which makes it difficult to detect gearbox faults by traditional time domain analysis and frequency domain analysis. Thus, some time–frequency analysis methods are used for gearbox fault detection. Wavelet transform is a commonly used time–frequency analysis method, which is widely used in gearbox fault diagnosis (Yu et al. 2017). However, the effect of wavelet transform depends on the selection of suitable wavelet basis function, which limits the application of wavelet transform (Honorio et al. 2012). Norden E Huang proposed Hilbert Huang transform for the non-linear and non-stationary signals, and the Empirical Mode Decomposition (EMD) is the key technique of the Hilbert Huang transform. EMD is a self-adaptive analysis technique which can decompose non-stationary signals into a series of intrinsic mode functions (IMFs) (Li et al. 2017). However, EMD still has many shortcomings, such as the criterion of IMF, over-decomposition, end effect and modal mixing. To overcome these inherent defects, Peng et al. (2005) combines Wavelet Packet Decomposition (WPD) with EMD to ensure that each IMF obtained by EMD is a single component. Yang (2008) uses band-pass filter to preprocess the mechanical fault signal and then decomposes the signal with EMD, which can restrain many shortcomings of EMD. Tang et al. (2012) uses the improved blind source separation method to suppress the modal mixing effect of EMD. Wu and Huang (2009) proposes the Ensemble Empirical Mode Decomposition (EEMD) for the problem of modal aliasing in EMD. EMD is used to decompose the signal in this work, and then IMFs with large kurtosis are selected to reconstruct to enhance the fault characteristics.

Therefore, the deconvolution technique is proposed to identify the fault of rotating machinery. The minimum entropy deconvolution (MED) is based on searching for a linear time-invariant filter which maximizes kurtosis of the filtered signal (Obuchowski et al. 2016). Compared with the traditional deconvolution method, MED does not need any assumptions and prior knowledge. It is an iterative method which can construct filters adaptively to find sparse spikes with simple characteristics (Cabrelli 1984). The method has been applied to gearbox faults detection successfully by Endo and Randall (2007, 2009). Meanwhile, the MED also can be used to identify the rolling bearings fault (Jiang et al. 2012; Sawalhi et al. 2007), and it proved to be an effective method. Nevertheless, some drawbacks of MED emerged during application to rotating machinery fault diagnosis. One of drawbacks is that the use of MED may produce spurious impulse whatever the signal is a fault signal or a white noise signal. The other one is that MED may not obtain optimal results due to iterative operations.

In view of these problems of MED, GL. Mcdonald proposed Maximum Correlated Kurtosis Deconvolution (MCKD) for gearbox fault detection (McDonald et al. 2012). MCKD can solve the problems of MED mentioned above. But MCKD is also an iterative process, it is usually impossible to obtain the optimal filter, and the fault cycle needs to be known beforehand. In addition, extra signal resampling pretreatment is needed for non-integer fault cycle, which increases computational complexity and limits its practical application. Thus, GL. Mcdonald also proposed a new deconvolution method called Multipoint Optimal Minimum Entropy Deconvolution (MOMEDA) for gearbox fault detection (McDonald and Zhao 2017). The method solves the iterative problem and achieves good results. However, vibration signals collected from a mechanical system usually contain a large amount of noise. For this reason, it often affects the effect of the above method.

Thus, a fault detection method based on EMD and MOMEDA is proposed in this paper. Firstly, the vibration signal is decomposed to some IMFs by EMD. It is well known that kurtosis is an impulse index for vibration signal, and the kurtosis of the fault signal is usually greater than the kurtosis of the noise signal. Therefore, some large kurtosis components are selected from these IMFs to reconstruct the fault signal. Finally, the processed signals are processed by MOMEDA to achieve the purpose of fault detection. Experimental data on a gearbox with broken tooth are used to verify the performance of the proposed method.

The remains of this paper is organized as follows: Sect. 2 gives the theoretical background of the MED technique, MCKD technique and the proposed method. In Sect. 3, the performance of the described approach on experimental gearbox faulty data is presented. Finally, the conclusion of the paper is given in Sect. 4.

2 Theoretical background

2.1 Minimum entropy deconvolution

The minimum entropy deconvolution was originally proposed by Wiggins (1978) for extraction of seismic wave reflection parameters. Then the technology gradually expanded to other fields. The basic principle of MED is to design the optimal filter rely on the property that MED can enhance the impulse characteristic. After filtered, the pulse impulse component of the filtered signal is enhanced, and the calculation terminates when the maximum kurtosis value is reached.

Suppose that the input signal is $x(t)$, and the MED filter is $f(t)$. Thus, the output signal by using the MED filter is:

$$y(t) = x(t)f(t) \tag{1}$$

If the length of MED filter is L, the Eq. 1 can also be written as follows:

$$y(t) = \sum_{l=1}^{L} f(l)x(t-l) \tag{2}$$

The kurtosis is large for the pulse impulse in vibration signal. Therefore, the kurtosis value of the filtered signal is considered as the result function to evaluate the filtering effect. The result function is calculated in the following formula:

$$K(f(l)) = \frac{\sum_{t=1}^{N} y^4(t)}{\left(\sum_{t=1}^{N} y^2(t)\right)^2} \tag{3}$$

where the l equals 1, 2,……L. In order to obtain the maximum of $K(f(l))$, the derivative of filter coefficients f(l) for the above formula is obtained, and the derivative is equal to zero so that the solution is obtained. After deducing and simplifying, the following formula can be obtained:

$$\frac{\sum_{t=1}^{N} y^2(t)}{\sum_{t=1}^{N} y^4(t)} \sum_{t=1}^{N} \left(y^3(t) \frac{\partial y(t)}{\partial f(l)} \right) = \sum_{t=1}^{N} \left(y(t) \frac{\partial y(t)}{\partial f(l)} \right) \tag{4}$$

A, b, f are respectively equal to the following formula:

$$b = \frac{\sum_{t=1}^{N} y^2(t)}{\sum_{t=1}^{N} y^4(t)} \sum_{t=1}^{N} \left(y^3(t) d(t-l) \right) \tag{5}$$

$$A = \sum_{t=1}^{N} \sum_{p=1}^{L} \left(d(t-p) d(t-l) \right) \tag{6}$$

$$F = \sum_{p=1}^{L} f(p) \tag{7}$$

Then it can be obtained in matrix form:

$$b = AF \tag{8}$$

It also can be calculated as follows:

$$F = A^{-1}b \tag{9}$$

where b is a cross-correlation vector which is obtained by calculating the correlation between the input and output signals of the inverse filter; and A is the Toeplitz autocorrelation vector that is a weighted summation of the autocorrelations of the input signals; the F is the coefficients vector for the desired inverse filter.

The implementation steps of MED can be summarized as follows:

Step 1 Compute the autocorrelation vector A
Step 2 Initialize the MED filter coefficients
Step 3 The output signal is calculated by using MED filter
Step 4 Calculate the cross-correlation matrix b according to the Eq. 8
Step 5 Compute the filter coefficients rely on Eq. 9
Step 6 Calculate the termination condition of the iteration as follows:

$$\delta = \frac{\sum_{t=1}^{N} y^{(i)4}(t)}{\left(\sum_{t=1}^{N} y^{(i)2}(t)\right)^2} - \frac{\sum_{t=1}^{N} y^{(i-1)4}(t)}{\left(\sum_{t=1}^{N} y^{(i-1)2}(t)\right)^2} \tag{10}$$

where i is the number of iterations, the iteration process will terminate when the variation of the kurtosis value between the iterations is lower than the threshold value.

2.2 Maximum correlated Kurtosis deconvolution

The MCKD algorithm was putted forward to emphasize the periodic pulse components for the signal with noise. The evaluation criterion of this method is to maximize the correlation kurtosis. Suppose that the signal collected by sensor is:

$$x_n = h_n * y_n + e_n \tag{11}$$

where x_n is the original fault signal; h_n is the response of the system transmission path; y_n is the failure periodic impact component; e_n is the noise signal.

The h_n masked the fault cycle impulse of the x_n, and the correlation kurtosis becomes smaller. The purpose of the MCKD algorithm is use the deconvolution to highlight the fault impact components, which is hidden in the raw signal. The key of the MCKD method is to search a finite length unit impulse response filter f. The filter can detect the original pulse signal $x(n)$ of the collected signal y_n, and the specific calculation process is shown as follows:

$$y_n = x_n * f_l \tag{12}$$

The objective function of MCKD is the maximum correlation kurtosis. Firstly, the correlation kurtosis is defined as follows:

$$CK_M(T) = \frac{\sum_{n=1}^{N} \left(\prod_{m=0}^{M} y_{n-mT} \right)^2}{\left(\sum_{n=1}^{N} y_n^2 \right)^{M+1}} \tag{13}$$

wherein M is the quantity of sequential pulses, which is to be deconvolution. The T is the separation cycle of these pulses. Thus, the objective function is shown as follows:

$$MCKD_M(T) = \max_{f_l} \frac{\sum_{n=1}^{N} \left(\prod_{m=0}^{M} y_{n-mT}\right)^2}{\left(\sum_{n=1}^{N} y_n^2\right)^{M+1}} \tag{14}$$

To maximize the correlation kurtosis, we solve

$$\begin{aligned}\frac{dCK_m(T)}{df_l} &= 0 = 2 \parallel y \parallel^{-2M-2} \\ &\sum_{n=1}^{N}\left[\left(\prod_{m=0}^{M} y_{n-mT}\right)^2 \left(\sum_{m=0}^{M} \frac{x_{n-mT-k+1}}{y_{n-mT}}\right)\right] \\ &- 2(M+1) \parallel y \parallel^{-2M-4} \sum_{n=1}^{N}\left(\left(\prod_{m=0}^{M} y_{n-mT}\right)^2\right) \\ &\sum_{n=1}^{N} y_n x_{n-k+1}\end{aligned} \tag{15}$$

The result of the filter is shown as follows by simplification and representation in matrix form.

$$f = \frac{\parallel y \parallel^2}{2 \parallel B \parallel^2} (X_0 X_0^T)^{-1} \sum_{n=0}^{M} X_{mT} A_m \tag{16}$$

$$A_m = \begin{bmatrix} y_{1-mT}^{-1}(y_1^2 y_{1-T}^2 \cdots y_{1-MT}^2) \\ y_{2-mT}^{-1}(y_2^2 y_{2-T}^2 \cdots y_{2-MT}^2) \\ \vdots \\ y_{N-mT}^{-1}(y_N^2 y_{N-T}^2 \cdots y_{N-MT}^2) \end{bmatrix},$$

$$B = \begin{bmatrix} y_1 y_{1-T} \cdots y_{1-MT} \\ y_1 y_{1-T} \cdots y_{1-MT} \\ \vdots \\ y_N y_{N-T} \cdots y_{N-MT} \end{bmatrix}$$

The array $X_0 X_0^T$ is the Toeplitz autocorrelation array of x_n and the inverse $(X_0 X_0^T)^{-1}$ is supposed to exist. The flow of the MCKD algorithm is shown as follows:

Step 1 Initialization deconvolution period T, number of sequential M and the length of filter
Step 2 Calculate the $X_0 X_0^T$ and X_{mT} of the input signal
Step 3 Calculate the filtered signal y
Step 4 Calculate the A_m and B from the filtered signal
Step 5 Update filter coefficient fl
Step 6 If the $\Delta CK_m(T)$ is less than the threshold, the iteration is ended, or 3–5 steps are repeated
Step 7 Calculate the period T of the final filtered signal

2.3 Multipoint optimal minimum entropy deconvolution

One drawback of MED is that the coefficients of the filter have been determined when iteration is performed. To overcome this shortcoming, Cabrelli (1985) has proposed a new norm called D norm, which is mainly used to deconvolution pulse signals. The D-Norm is shown as follows:

$$D(y) = \max_{k=1,2,\ldots,N} \frac{|y_k|}{\|y\|} \tag{17}$$

On this basis, Geoff L. McDonald proposed the concept of Muti D-Norm and introduced a new algorithm called Multipoint Optimal Minimum Entropy Deconvolution Adjusted (MOMEDA). The Muti D-Norm is formulated as the following:

$$MDN(y,t) = \frac{1}{\|t\|} \frac{t^T y}{\|y\|} \tag{18}$$

where the t is a constant vector in the deconvolution, which determines the location and weight of the goal impulse. The objective function of MOMEDA is to make the MDN maximum as following:

$$\max_f MDN(y,t) = \max_f \frac{t^T y}{\|y\|} \tag{19}$$

To maximize the MDN, we solve

$$\frac{d}{df}\left(\frac{t^T y}{\|y\|}\right) = \frac{d}{df}\left(\frac{t_1 y_1}{\|y\|}\right) + \frac{d}{df}\left(\frac{t_2 y_2}{\|y\|}\right) + \cdots + \frac{d}{df}\left(\frac{t_{N-L} y_{N-L}}{\|y\|}\right) \tag{20}$$

After simplification,

$$\begin{aligned}\frac{d}{df}\left(\frac{t^T y}{\|y\|}\right) &= \|y\|^{-1}(t_1 M_1 + t_2 M_2 + \cdots + t_{N-L} M_{N-L}) \\ &- \|y\|^{-3} t^T y X_0 y\end{aligned} \tag{21}$$

$$X_0 = \begin{bmatrix} x_L & x_{L+1} & x_{L+2} & \cdots & x_N \\ x_{L-1} & x_L & x_{L+1} & \cdots & x_{N-1} \\ x_{L-2} & x_{L-1} & x_L & \cdots & x_{N-2} \\ \vdots & \vdots & \vdots & \ddots & \vdots \\ x_1 & x_2 & x_3 & & x_{N-L+1} \end{bmatrix}$$

where the $M_k = [x_{k+L-1}, x_{k+L-2} \cdots x_k]^T$, then the equation can be written as follows.

$$\frac{d}{df}\left(\frac{t^T y}{\|y\|}\right) = \|y\|^{-1} X_0 t - \|y\|^{-3} t^T y X_0 y \tag{22}$$

The above formula is equal to zero and can be obtained:

$$\|y\|^{-1} X_0 t - \|y\|^{-3} t^T y X_0 y = 0 \tag{23}$$

Since $y = X_0^T f$ and assuming $(X_0 X_0^T)^{-1}$ exists, the Eq. 21 becomes:

$$\frac{t^T y}{\|y\|^2} f = (X_0 X_0^T)^{-1} X_0 t \tag{24}$$

Hence the filter can be calculated as following:

$$f = (X_0 X_0^T)^{-1} X_0 t \tag{25}$$

Where the length of vector t is $(N - L + 1)$, it is same as the output signal.

2.4 Empirical mode decomposition

EMD is an adaptive signal processing method for nonlinear and non-stationary signals. The precondition of the method is that the signal is composed of a series of intrinsic mode functions (IMFs). Moreover, each of IMFs is required to satisfy the following conditions (Huang et al. 1998):

(1) The extreme points and zero crossing points of the entire IMF signal must be equal or at least one difference (Yang et al. 2006).
(2) For any data point, the envelope average value of its local maximum and minimum must be zero, that is, the local envelope signal is symmetrical with respect to the time axis (Cheng et al. 2006).

EMD is based on the premise that any signal is composed of many different IMFs. The process of decomposing a given signal x (t) into a number of IMFs can be summarized as follows:

(1) Indentify all the local extrema, the upper envelope of the signal $x(t)$ is determined according to its local maxima. Similarly, the lower envelope of the signal can be obtained rely on the local minima. Then calculate the mean of upper and lower envelope value as the m_1.
(2) The first component h_1 is the difference between the signal $x(t)$ and m_1, the formula is as follows:

$$x(t) - m_1 = h_1 \tag{26}$$

h_1 will be the first IMF when it meets the above two requirements.

(3) When h_1 does not meet the above two requirements, it will be used as the raw signal to duplicate the above first two steps.

$$h_1 - m_{11} = h_{11} \tag{27}$$

Then repeat operation k times until h_{1k} becomes an IMF shown as follows:

$$h_{1(1-k)} - m_{1k} = h_{1k} \tag{28}$$

Then make c_1 equal to h_{1k} as the first IMF of signal.

(4) The signal r_1 is obtained after the signal c_1 is removed from the raw signal.

$$r_1 = x(t) - c_1 \tag{29}$$

The r_1 repeats the above processes as a new raw signal and the second IMF can be obtained. A raw signal can get several IMFs by repeating the above operation, the decomposition is terminated until the remaining signal r_n is monotonic.

Therefore, the raw signal $x(t)$ can be written as follows.

$$x(t) = \sum_{i=1}^{n} c_i + r_n \tag{30}$$

$c_1, c_2, \ldots, c_n$ represent IMFs with different frequency bands, which are arranged from high to low. Each frequency band contains different frequency components and they varies according to the raw signal $x(t)$. The residual signal represents the overall trend of the raw signal $x(t)$.

3 Proposed method

The proposed method of fault detection based on EMD-MOMEDA is illustrated in this section. As known, the MOMEDA is an efficient technique for detecting faults of mechanical parts. However, the working environment of the mechanical system is usually complex. For this reason, the signals measured by accelerometers, which installed on the rotating machinery, always contains large amounts of random noise. Furthermore, the signal is also doped into the noise signal during the acquisition process. These

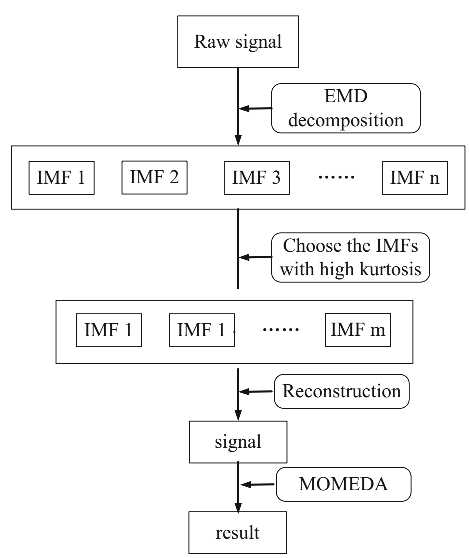

Fig. 1 Diagram of the proposed method

causes affect the signal processing effect of the MOMEDA method. To overcome this problem, EMD is proposed to process the raw signal to eliminate noise interference, the decomposition and reconstruction of signals using EMD can eliminate the influence of random components. Therefore, the method of fault detection based on EMD-MOMEDA is proposed in this work.

The operation flow of the new method is shown as Fig. 1.

4 Experimental data analysis

In order to make a qualitative validation of the mentioned method, the gearbox preset fault experiments was carried out to investigate the effectiveness of the new method.

4.1 Case study 1

4.1.1 Experimental setup

The test rig is composed of a 4 kW stepless speed motor, a parallel shaft gearbox, a speed torque sensor, a magnetic powder brake and signal acquisition system. The overall structure of the test bed is presented in Fig. 2. The magnetic particle brake can provide the load for the experiment. As shown in Fig. 3, the test gearbox is equipped with a set of four gears and three shafts. The input shaft of the gearbox is driven through stepless speed motor, the power is transmitted from the input shaft to the output shaft by the intermediate shaft. The magnetic powder brake can provide load, which is connected with the output end of the gearbox through a coupling. Thus the conservation of energy is achieved. In the experiment, three different degrees of broken teeth are implanted in gear 2 of intermediate shaft. The width of broken teeth fault is 2 mm, 5 mm and 10 mm respectively as shown in Fig. 4. Experiments are carried out to test the performance of each degree broken tooth fault under different speed and load combinations. Shaft rotational speed is 800 rpm, 1000 rpm and 1200 rpm, the loads are 10 Nm, 15 Nm and 20 Nm respectively. The signal acquisition system consists of a computer, four

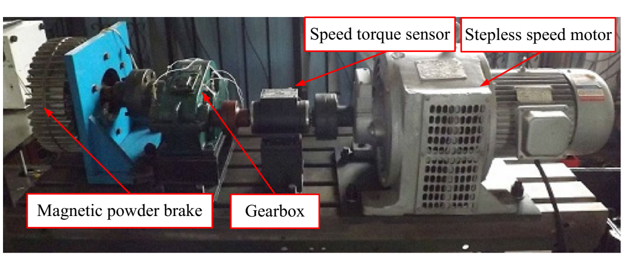

Fig. 2 Gearbox implanted fault test-rig

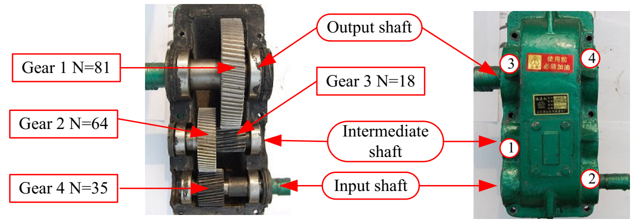

Fig. 3 Gearbox structure and sensor position

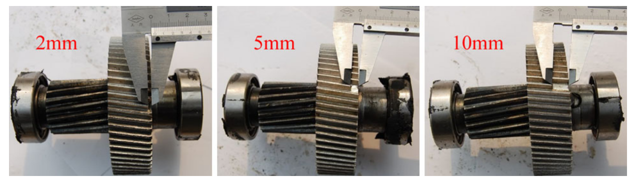

Fig. 4 Broken tooth fault on gear 2 with different degrees

3065B4 piezoelectric accelerometer produced by DYTRAN company, a PXI-1031 chassis of NI company, data acquisition card and Labview software. The accelerometers were mounted on the outside of the gearbox such as the location of the digital mark shown in Fig. 3. Data is sampled at 20 kHz per channel for six seconds.

As shown in the Fig. 3, the number of the gear teeth has been known. Thus, the fault frequency of broken tooth is calculated and given in Table 1.

4.1.2 Experiment result analysis

In this paper, the data of 2 mm broken tooth fault under the condition of 800 rpm and 10Nm is used to investigate the effectiveness of proposed method. First of all, the traditional Fourier spectrum and cepstrum are used to analyze the fault signal and the normal state signal. The Fourier spectrum and cepstrum are shown as Figs. 5 and 6. As shown in the Fig. 5, there is no significant difference between normal signal spectrum and fault signal spectrum, no fault frequency component is found in fault signal spectrum. It is illustrate that the Fourier spectrum is difficult to identify the fault accurately. As shown in the Fig. 6, the cepstrum of fault signal also has no cycle time corresponding to fault frequency. Therefore, it is difficult to detect the gear fault only by traditional spectrum analysis. Then the method proposed in this paper is used to detect gear faults.

Table 1 Basic size and style requirements

Speed	800 rpm	1000 rpm	1200 rpm
Fault frequency	7.29 Hz	9.11 Hz	10.94 Hz

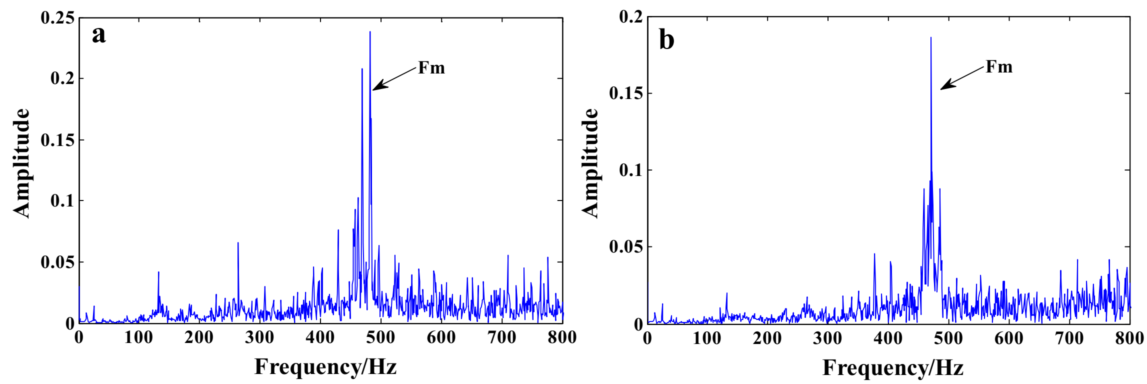

Fig. 5 Fourier spectrum of normal signal and fault signal **a** normal signal, **b** fault signal

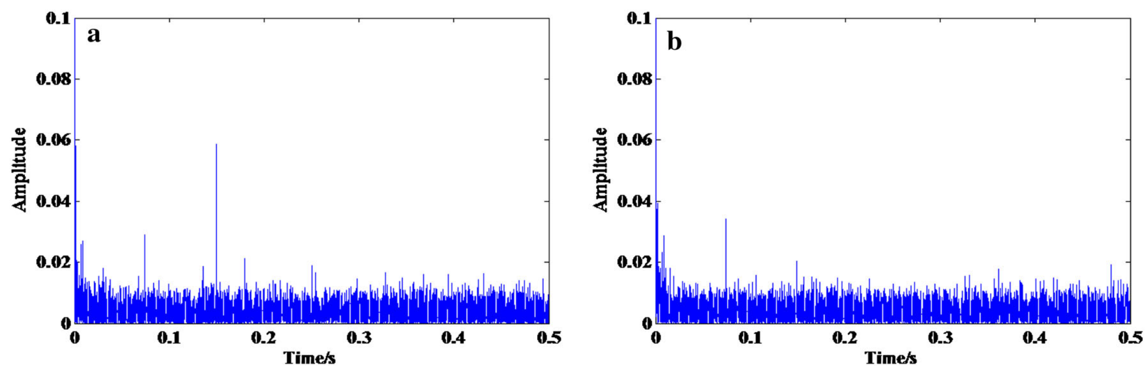

Fig. 6 Cepstrum of normal signal and fault signal **a** normal signal, **b** fault signal

Firstly, the raw signal is decomposed to several IMFs by EMD. The result of signal decomposition is presented in Fig. 7. After applying the EMD to the data, the IMFs needs to be selected and reconstructed. In these IMFs, only some IMFs that contain the fault impact signals are useful. The signal components contained in the remaining IMFs are useless for fault diagnosis, such as random noise. Because kurtosis is widely used to reflect the characteristic of the shock, the kurtosis of all the IMFs are calculated are given in Fig. 8. Select IMF with kurtosis above 3.5 to reconstruct the signal. As shown in the Fig. 8, IMF 2, IMF 4, IMF 5, IMF 6 and IMF 7 are chosen to reconstruct the signal for the fault diagnosis. The reconstructed signal is processed by MOMEDA and the result is shown in Fig. 9. In the Fig. 9, the T is sample count between two consecutive fault impulses. Thus, the period of fault impulse can be computed by T and sample rate. The fault impulse frequency can be calculated by period. After calculation, the fault impulse frequency is 7.3 Hz approximately. The fault impulse frequency is consistent with the fault characteristic frequency calculated above. Therefore, the broken tooth fault can be diagnosed accurately by using proposed method in this paper, then the effectiveness of the method is proved.

To illustrate the influence of EMD in the method, the signal also be processed by only using MOMEDA and the result is presented in the Fig. 10. As shown in the figure, the fault impulse can not be found obviously. Therefore, it is necessary to carry out EMD before using MOMEDA for diagnosis.

In order to further prove the validity of the proposed method, a comparison of MCKD, MED and proposed method is also carried out on the same signal. The performance of the MCKD is shown in the Fig. 11, there are two fault impulses can be found in the figure. However, it is difficult to argue that the fault impact has periodicity. Thus, the broken tooth fault of the gear can not be identified accurately. Figure 12 shows the process result by using MED, and the fault impulse is blurred and confused in the figure. In view of this, the broken tooth fault can not be detected.

The data of 5 mm and 10 mm broken tooth fault under the condition of 800 rpm and 10Nm are used to further prove the effectiveness of the EMD-MOMEDA. The processing results are shown in the Figs. 13 and 14 below. As can be seen from the graphs, the impact pulses can be clearly highlighted from the fault signal by used proposed method. Therefore, the validity of the method can be further proved.

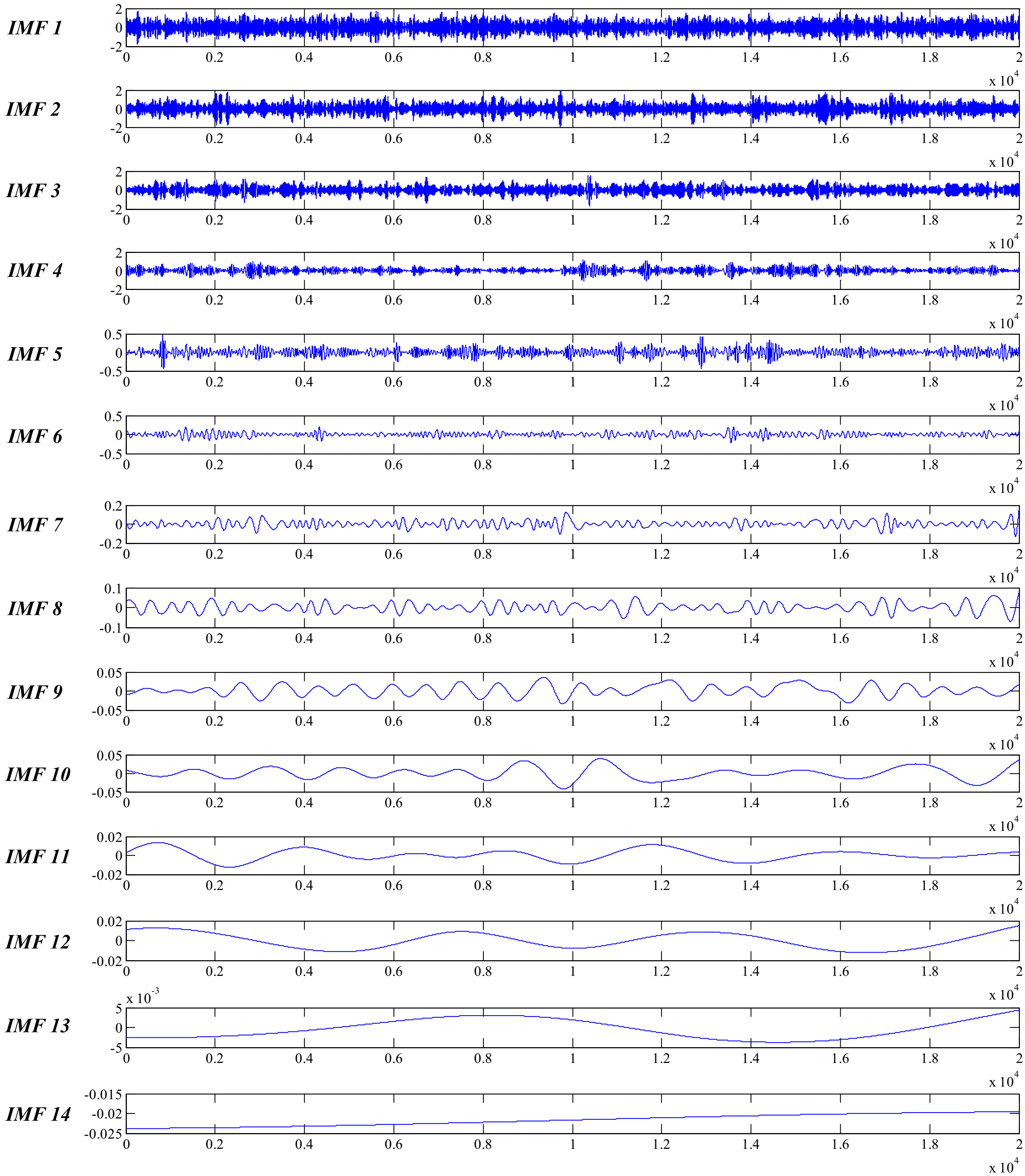

Fig. 7 EMD decomposition results

The length of the filter is the key factor that affects the effect of EMD-MOMEDA. For the same signal, the EMD-MOMEDA is used for processing with different length filter, the result is shown in Fig. 15. As can be seen from the figure, with the increasing of filter length, the impulses of signal become stronger and clearer gradually. Thus, the conclusion is drawn that the length of the filter can enhance the effect of the proposed method.

The Fig. 16 is shown the result of using MCKD with different length filter for the same signal. As shown in the

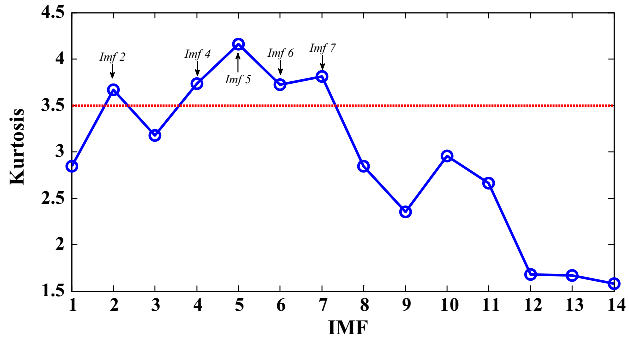

Fig. 8 Kurtosises of all IMFs

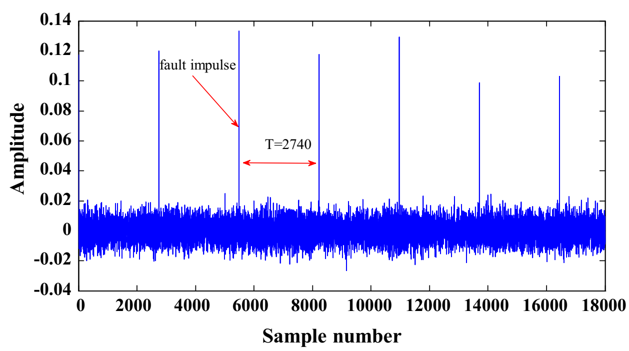

Fig. 9 The result of 2 mm broken tooth data processed by proposed method

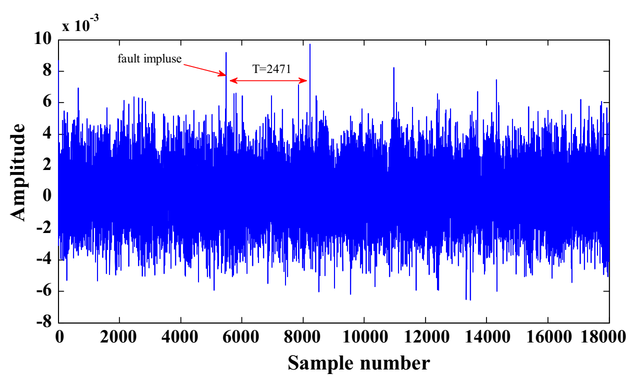

Fig. 10 The result of 2 mm broken tooth data processed by MOMEDA

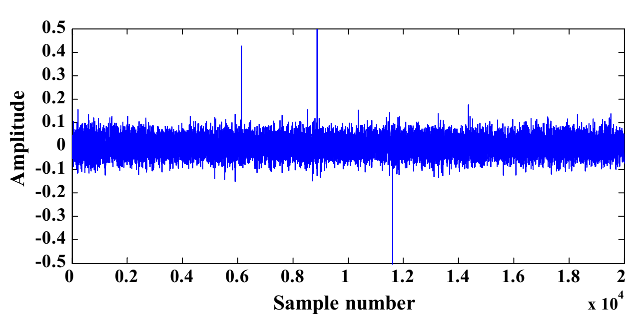

Fig. 11 The result of 2 mm broken tooth data processed by MCKD

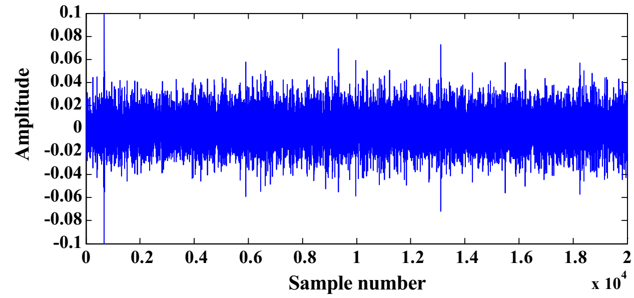

Fig. 12 The result of 2 mm broken tooth data processed by MED

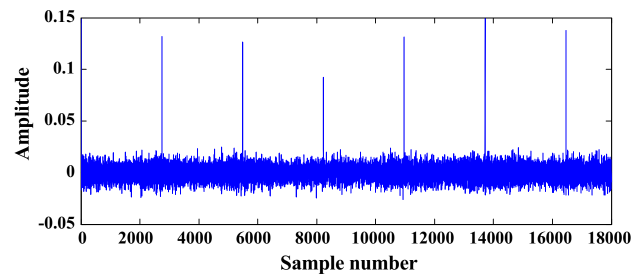

Fig. 13 The result of 5 mm broken tooth data processed by proposed method

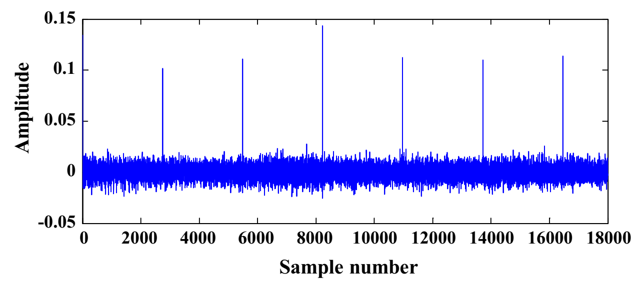

Fig. 14 The result of 10 mm broken tooth data processed by proposed method

Fig. 16, increasing the length of the filter can reduce the influence of noise on impact pulse. The Fig. 17 is shown the result of using MED with different length filter for the same signal. As can be seen from the figure, the length of filter can also affect the effect of the MED, but it is not obvious.

4.2 Case study 2

In order to further prove the feasibility of the proposed method, another preset fault experiment of gearbox was carried out. As shown in the Fig. 18, the test rig is composed of a stepless speed motor, a parallel shaft gearbox, a speed torque sensor, two vibration sensors, a magnetic powder brake and signal acquisition system. The structure of the experimental gearbox and the gear with broken tooth are shown in the Fig. 19. Sampling rate is 20,480 Hz and

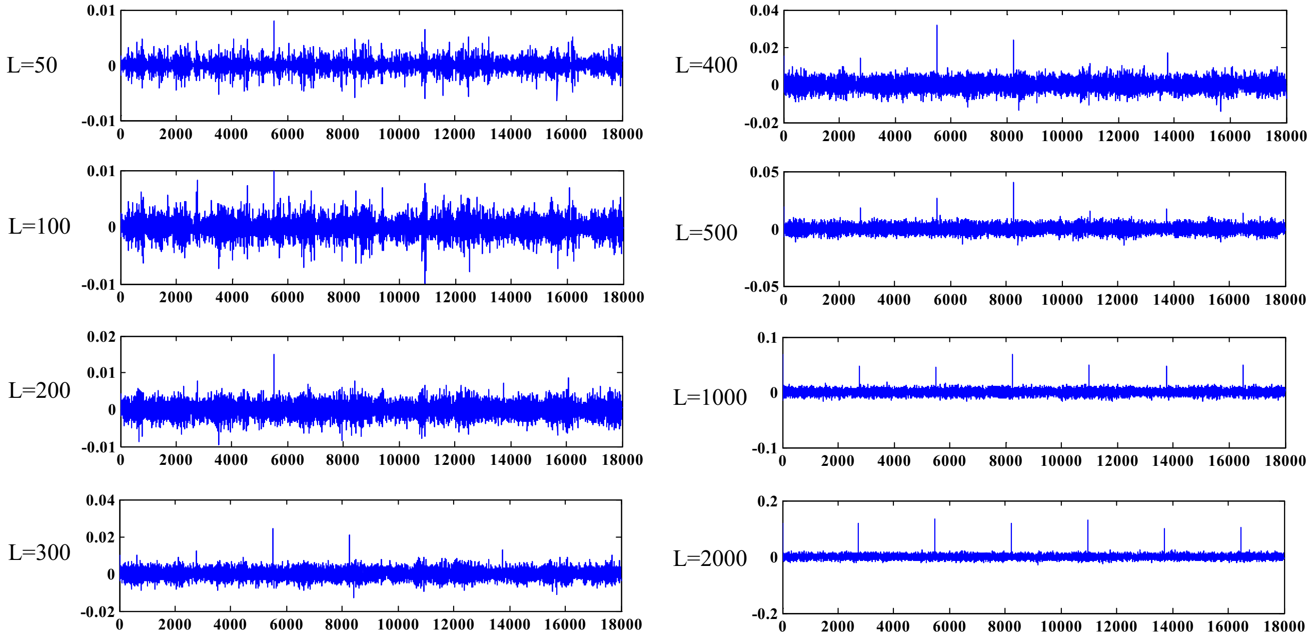

Fig. 15 The result of 2 mm broken tooth data using EMD-MOMEDA with different length filter

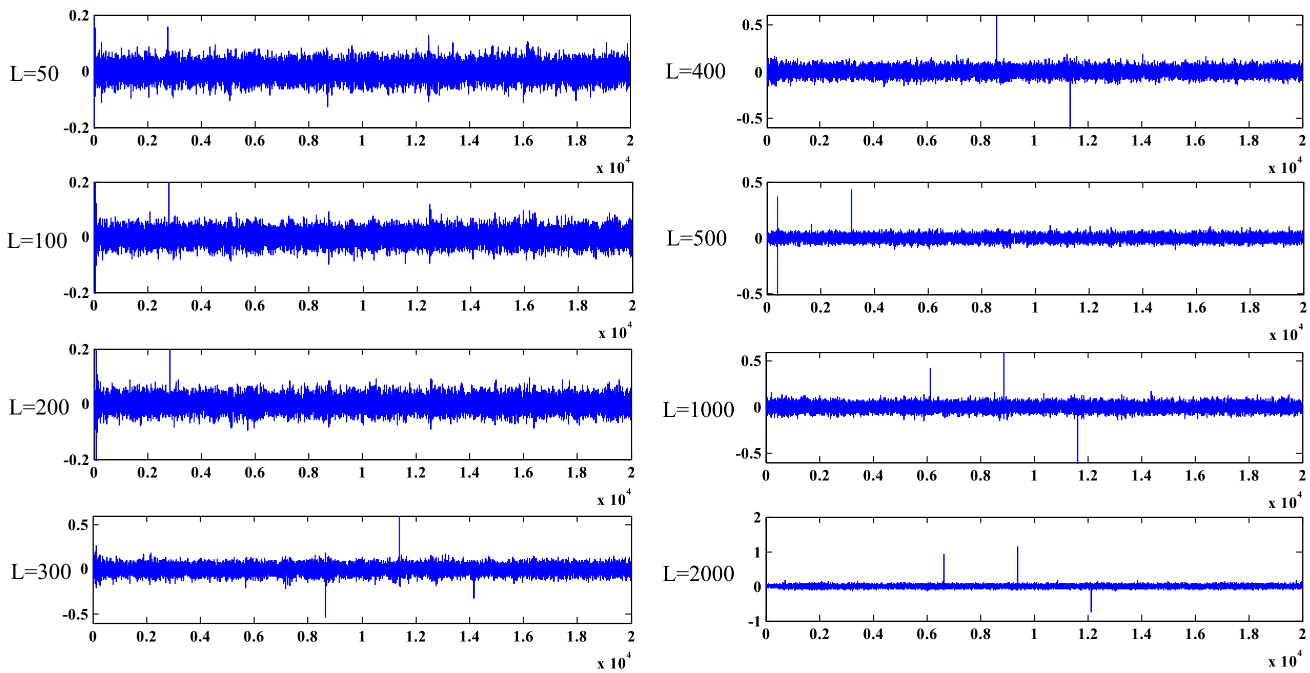

Fig. 16 The result of 2 mm broken tooth data using MCKD with different length filter

sampling time is 9.6 s. The Fig. 20 displays the time domain waveform of raw signal for broken tooth fault. The rotation frequency is 20 Hz in the experiment. The fault frequency of broken tooth fault is 10.38 Hz. After calculation, the period of fault impact is 1973 sample points.

After processing by the proposed method, the results are shown in Fig. 21. As shown in the Fig. 21, there are periodic shock characteristics in the result graph. The fault impulse frequency is consistent with the fault characteristic frequency calculated above. Therefore, the broken tooth fault can be diagnosed accurately by using proposed method in this paper and the effectiveness of the method is proved.

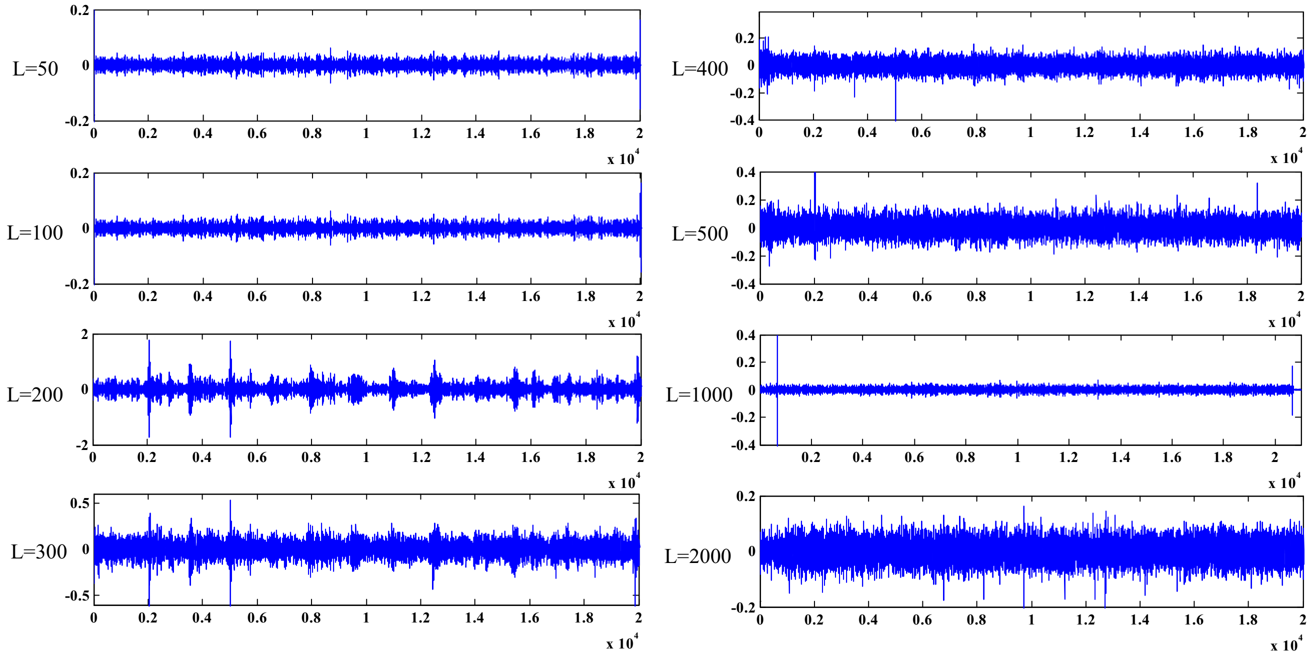

Fig. 17 The result of 2 mm broken tooth data using MED with different length filter

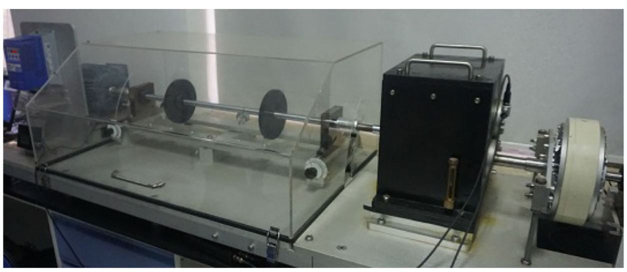

Fig. 18 Gearbox implanted fault test-rig

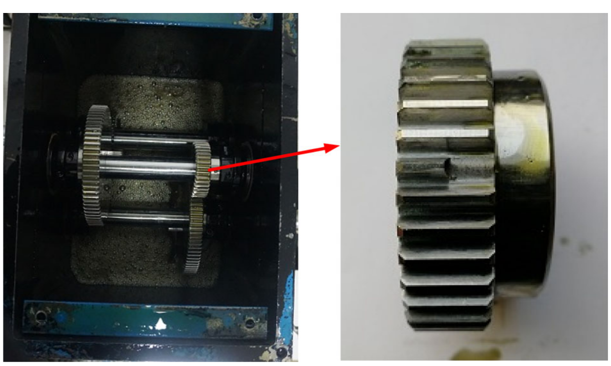

Fig. 19 Gearbox structure and gear with broken tooth fault

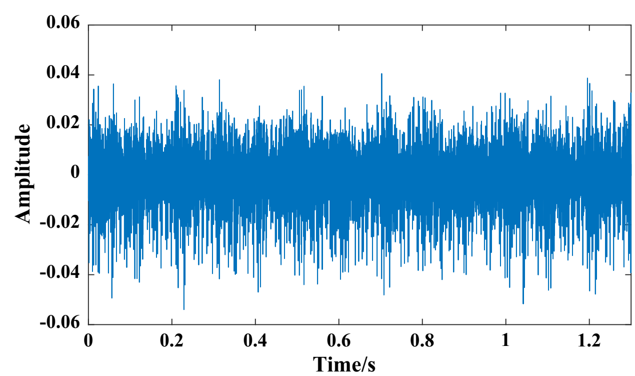

Fig. 20 Waveform of raw signal for broken tooth fault

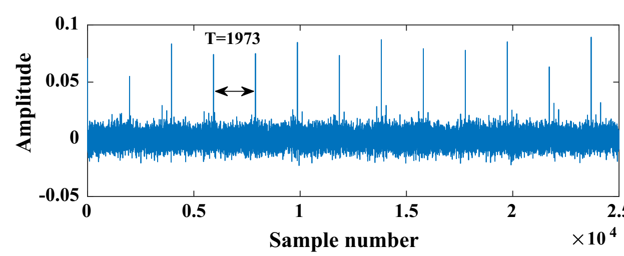

Fig. 21 The result of broken tooth data processed by proposed method

5 Conclusions

In this work, a novel hybrid method based on EMD and MOMEDA is proposed to fault detection for gearbox. In the proposed method, EMD is used to decompose the raw signal to get IMFS and then select the IMFs with large kurtosis value to reconstruct the signal. Then the reconstructed signal is processed by MOMEDA to realize fault detection. In order to illustrate the availability of the proposed approach, a gearbox preposition fault experiment is carried out. This combined approach is applied to experimental signal. The experimental results illustrate that the method is effective for fault detection of gearbox. The experimental results also show that the method is more competitive for fault detection of gearbox compared with traditional methods such as Fourier spectrum, cepstrum, MOMEDA, MCKD and MED. The influence of different filter length on the proposed method is also analyzed, with the increasing of filter length, the effect of the proposed method is better.

References

Cabrelli CA (1984) Minimum entropy deconvolution and simplicity: a noniterative algorithm. Geophysics 50:394–413

Cabrelli CA (1985) Minimum entropy deconvolution and simplicity: a noniterative algorithm. Geophysics 50(3):394–413

Cheng J, Dejie Yu, Yang Yu (2006) A fault diagnosis approach for roller bearing based onEMD method and AR model. Mech Syst Signal Process 20:350–362

Endo H, Randall RB (2007) Enhancement of autoregressive model based gear tooth fault detection technique by the use of minimum entropy deconvolution filter. Mech Syst Signal Process 21:906–919

Endo H, Randall RB, Gosselin C (2009) Differential diagnosis of spall cracks in the gear tooth fillet region: experimental validation. Mech Syst Signal Process 23:636–651

Feng Z, Chen X, Liang M (2016) Joint envelope and frequency order spectrum analysis based on iterative generalized demodulation for planetary gearbox fault diagnosis under non-stationary conditions. Mech Syst Signal Process 76:242–264

Golafshan R, Sanliturk KY (2015) SVD and Hankel matrix based de-noising approach for ball bearing fault detection and its assessment using artificial faults. Mech Syst Signal Process 70–71:36–50

Gu D, Kim JG, An YS, Choi BK (2011) Detection of faults in gearboxes using acoustic emission signal. J Mech Sci Technol 25(5):1279–1286

Halim EB, Shoukat Choudhury MAA, Shan SL, Zuo MJ (2008) Time domain averaging across all scales: a novel method for detection of gearbox faults. Mech Syst Signal Process 22:261–278

Hamilton A, Quail DF (2011) Detailed state of the art review for the different on-line/in-line oil analysis techniques in context of wind turbine gearboxes. ASME J Tribol 133(4):1–17

Hong L, Dhupia JS (2014) A time domain approach to diagnose fearbox fault based on measured vibration signals. J Sound Vib 333:2164–2180

Hong L, Dhupia JS, Sheng S (2014) An explanation of frequency features enabling detection of faults in equally spaced planetary gearbox. Mech Mach Theory 73:169–183

Honorio BCZ, Mmond RD, Vidal AC, Leite EP (2012) Well log denoising and geological enhancement based on discrete wavelet transform and hybrid thresholding. Energy Explor Exploit 30:417–433

Huang NE, Shen Z, Long SR et al (1998) The empirical mode decomposition and the Hilbert spectrum for non-linear and non-stationary time series analysis. Proc R Soc Lond A 454:903–995

Jiang R, Chen J, Dong G et al (2012) The weak fault diagnosis and condition monitoring of rolling element bearing using minimum entropy deconvolution and envelop spectrum. J Mech Eng Sci 227:1116–1129

Li B, Zhang X, Jili W (2017) New procedure for gear fault dectection and diagnosis using instantaneous angular speed. Mech Syst Signal Process 85:415–428

Lim GM, Bae DM, Kim JH (2014) Fault diagnosis of rotating machine by thermography method on support vector machine. J Mech Sci Technol 28(8):2947–2952

McDonald GL, Zhao Q (2017) Multipoint optimal minimum entropy deconvolution and convolution fix: application to vibration fault detection. Mech Syst Signal Process 82:461–477

McDonald GL, Zhao Q, Zuo MJ (2012) Maximum correlated Kurtosis deconvolution and application on gear tooth chip fault detection. Mech Syst Signal Process 33:237–255

McFadden PD (1991) A Technique for calculating the time domain averages of the vibration of the individual planet gears and the sun gear in an epicyclic gearbox. J Sound Vib 144(1):163–172

McFadden PD, Smith JD (1985) A signal processing technique for detecting local defects in a gear from the signal average of the vibration. Proc Inst Mech Eng Part C J Mech Eng Sci 199(43):287–292

Obuchowski J, Zimroz R, Wylomanska A (2016) Blind equalization using combined skewness-kurtosis criterion for gearbox vibration enhancement. Measurement 88:34–44

Peng ZK, Tse PW, Chu FL (2005) An improved Hilbert-Huang transform and its application in vibration signal analysis. J Sound Vib 286:187–205

Samuel PD, Pines DJ (2005) A review of vibration-based techniques for helicopter transmission diagnostics. J Sound Vib 282:475–508

Sawalhi N, Randall RB, Endo H (2007) The enhancement of fault detection and diagnosis in rolling element bearings using minimum entropy deconvolution combined with spectral kurtosis. Mech Syst Signal Process 21:2616–2633

Tang BP, Dong SJ, Song T (2012) Method for eliminating mode mixing of empirical mode decomposition based on revised blind source separation. Signal Process 92:248–258

Wiggins RA (1978) Minimum entropy deconvolution. Geoexploration 16(1–2):21–35

Wu ZH, Huang NE (2009) Ensemble empirical mode decomposition: a noise assisted data analysis method. Adv Adapt Data Anal 13:1–41

Yang WX (2008) Interpretation of mechanical signals using an improved Hilbert–Huang transform. Mech Syst Signal Process 22:1061–1071

Yang Yu, Dejie Yu, Cheng J (2006) A roller bearing fault diagnosis method based on EMD energy entropy and ANN. J Sound Vib 294:269–277

Yu K, Lin TR, Tan JW (2017) A bearing fault diagnosis technique based on singular values of EEMD spatial condition matrix and Gath-Geva clustering. Appl Acoust 121:33–45